Positron Emission Tomography agent for Non-Invasive Imaging of Antiretroviral Drug Penetration and Kinetics In Vivo

Michele Di Mascio*[1], Sharat Srinivasula[2], Matt Collins[3], Esther Lim[4], Lily Cheng[1], Dale Kiesewetter[5]

* Biostatistics Research Branch, NIAID, NIH. 6700B, Rockledge Drive, MSC 7609, Bethesda, Maryland 20892. Email: mdimascio@niaid.nih.gov

[1]NIAID, NIH, Bethesda, Maryland [2]SAIC-Frederick, Inc., Frederick, Maryland [3]Bioqual, Rockville, Maryland [4]University of Pennsylvania, Philadelphia, Pennsylvania [5]NIBIB, NIH, Bethesda, Maryland

Introduction

• The advent of Highly Active Antiretroviral Therapy (HAART) has led to striking decreases in AIDS related morbidity and mortality. Most HAART treated patients achieve viral suppression below 50 copies/ml of plasma within a few months from the start of the therapy. However, the cumulative risk of viral load failure has been estimated ~40% by 6 years from the initiation of therapy[1]

• Antiviral efficacy, dosing and toxicity of current HAART regimens are mostly derived from plasma or blood kinetics of anti-HIV drugs, with the blood comprising only 2% of total target cells in the body

• Tissue drug levels may substantially differ from corresponding plasma levels and drug distribution processes may be characterized by high inter-tissue variability, leading to suboptimal target site concentrations and the potential risk for therapeutic failures[2].

• Two major [not mutually exclusive] theories currently explain our inability to eradicate the virus: the drugs are not potent enough to prevent new infections and replenishment of viral reservoirs; or, the reservoirs are long-lived and no new infections of target cells are needed to sustain the residual level of virus [including drug resistant strains] observed in successfully treated patients[3,4,5]. Both theories do not exclude nor challenge the possibility that spatial heterogeneity in drug distribution can indeed accelerate the emergence of drug resistant strains

• Biopsies, for certain lymphoid organs, have frequently been utilized to measure drug concentrations in tissues. However, due to the invasive nature of these procedures, it is difficult, for obvious ethical reasons, to perform longitudinal analysis in the same subject, therefore limiting our knowledge of the in vivo kinetics of antiretroviral drugs during the years of chronic treatment in HIV-1 infected patients.

Here, we describe the tissue drug kinetics of Tenofovir (PMPA), a commonly used antiretroviral drug characterized by low metabolism in vivo[6], and its fluorine-18 radiolabeled analogue, a potential ligand for PET imaging.

Radioligands and pharmaceuticals

Racemic FPMPA, the fluorinated analog of PMPA was prepared following the literature procedure[7]. The radiochemical synthesis of racemic [^{18}F]FPMPA as well as the pure enantiomers (R)- and (S)-[^{18}F]FPMPA was performed by preparing chiral methanesulfonate precursors and conducting a fluorination. Product was purified by HPLC with high radiochemical purity of > 98%. Identity of the product was confirmed by co-elution of the obtained radiochemical product with the unlabeled standard on HPLC.

Inhibitory activity of R-PMPA (R enantiomer of PMPA), (RS)-FPMPA (racemic FPMPA), R-FPMPA and S-FPMPA was determined in rhesus monkey PBMC cells infected with SIVmac239 and human MT4 cells infected with $SHIV_{DH12R}$.

• R-PMPA inhibited SIVmac239 with an IC_{50} of 2.32μM (95% CI, 1.51 – 3.34) consistent with previously reported data[8].

• In two separate assays, (RS)-FMPMA inhibited SIVmac239 with IC_{50}'s of 4.85μM (95% CI, 3.8 – 6.67) and 6.66μM (95% CI, 5.1 – 8.9) which were not statistically significantly different.

• The observed increase in IC_{50} for racemic (RS)-FPMPA of approximately 2-3 fold compared to the IC_{50} of R-PMPA was highly statistically significant ($P < 0.001$) and is consistent with racemic drug being 1:1 ratio of two enantiomers, of which only one is active on the reverse transcriptase.

• S-FPMPA, but not the R-FPMPA, fully inhibited viral replication in human MT4 cells infected with $SHIV_{DH12R}$ with an estimated IC_{50} of 1.85μM (95% CI, 0.8 – 5.53).

Inhibitory activity

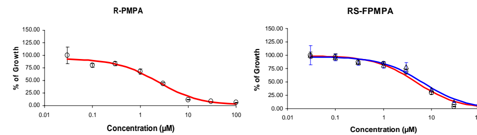

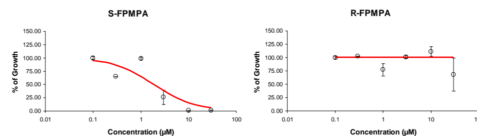

Inhibitory activity of R-PMPA and RS-FPMPA in macaque PBMC cells infected with SIVmac239; and of S-FPMPA and R-FPMPA in human MT4 cells infected with $SHIV_{DH12R}$

In vivo biodistribution study

• To test the similarity of biodistribution between PMPA and (S)-[^{18}F]FPMPA, we have performed a biodistribution study in rats with dual labeling. 12 male Sprague-Dawley rats (250-275 g) were co-injected intravenously with 5mg/kg of unlabeled PMPA, 5μCi of ^{14}C-PMPA and 200μCi of (S)-[^{18}F]FPMPA.

• The 12 rats were divided into 4 groups of 3 each and each group was dissected at 10, 30, 60 and 120 min post injection. Samples of submandibular left/right, popliteal left/right and mesenteric lymph nodes, spleen, lungs, kidney, liver, jejunum, colon, Peyers' patches, brain, femur, testes and blood were removed.

• The collected tissues were weighed in scintillation vials and [^{18}F]fluoride radioactive content of the whole-blood and various tissues was assayed using gamma counter.

• To determine ^{14}C activity, the samples were solubilized for 6 days in 1.5ml of solvable at room temperature. All samples were prepared further for scintillation counting by bleaching with 300μl of H_2O_2 and neutralizing with 50μl of 10N HCL, followed by addition of 16ml of scintillation cocktail, Aquasol. Samples were dark adapted and counted for 5 min each in a scintillation counter.

• Standards of 1:250 and 1:2500 of the injected dose were prepared and counted along with all samples. Background counts were subtracted from reported ^{18}F counts per minute (CPM) and ^{14}C disintegrations per minute (DPM) values.

• The injected counts were determined from the standard counts and the quantitative data expressed as percent of injected dose per gram of tissue (% ID/g) were determined by the following equation:

$$\% \text{ of ID/g of tissue} = \frac{\text{sample counts}}{\text{sample weight (g) x injected counts}} \times 100$$

The mean and the standard deviation of % ID/g were calculated for all samples in each group and for both ^{18}F and ^{14}C.

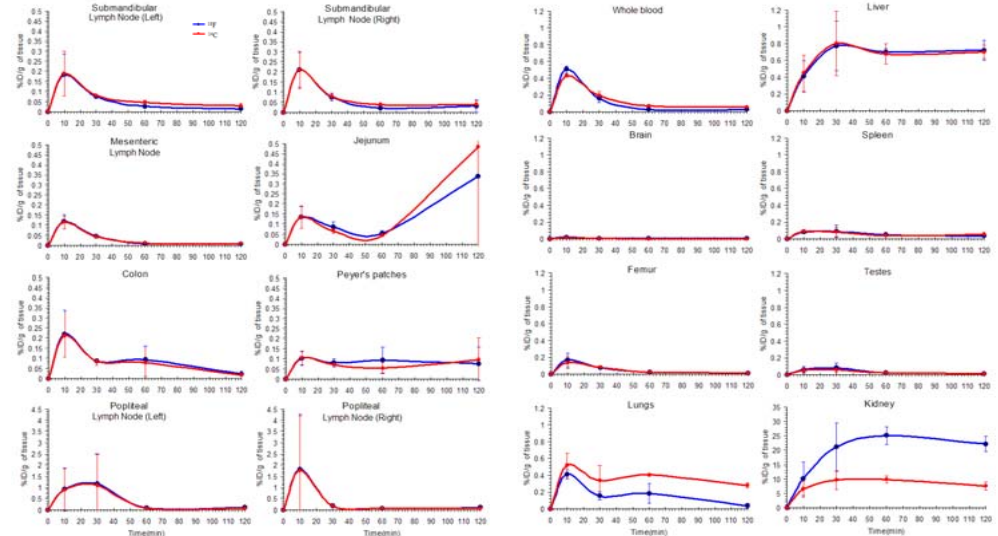

Percent of injected dose per gram of tissue (% ID/g) during time in the organs sampled. Blue line represent ^{18}F retention in tissues and Red represents ^{14}C retention.

Results

• In vivo biodistribution data (Figure) shows good overlapping of the ^{14}C-PMPA and (S)-[^{18}F]FPMPA distribution in several organs including femur (tissue with high avidity for unbound fluoride) suggesting that ^{18}F-fluoride is not a metabolite of FPMPA

• Interestingly, intra-subject variability of the trough drug concentration in certain tissues (Jejunum, Peyer's patches, c.v > 60%) is substantially higher than and not revealed by the blood compartment (c.v = 10%)

• Kinetics in the kidney shows drug accumulation, which might explain Tenofovir associated nephrotoxicity[9].

Future plans

• PET imaging

Conclusions

• (S)-[^{18}F]FPMPA is a candidate imaging probe for the distribution of Tenofovir in tissues in vivo.

• Drug penetration varies between anatomic compartments and subjects

• Potential areas of animal research and clinical investigation that could benefit from this technique are:

- Longitudinal analysis of drug kinetics during chronic treatment
- Drug interactions
- Drug volume distribution after topical administration of microbicide studies
- Generalization of the concept of efficacy of HAART regimens

References

1- Phillips A.N. et al. *AIDS* 2005; 19:487-94,

2-Kepler T.B. and Perelson A.S. *PNAS* 1998; 95:11514-11519

3-Zhang L. et al. *N Engl J Med* 1999; 340:1605-1613

4-Persaud D. et al. *J Clin Invest* 2000; 105:995-1003

5- Chun T.W. et al. *Nat Med* 2000; 6:757-761

6-Cundy et al. *A.A.C.* 1998; 42: p 687-690

7-Jindrich J. et al. Col Cze Che Com. 1992;57;1466-1482

8-Tsai C. C. et al. *Science* 1995; 270: 1197-1199.

9- Schaaf B. et al. *Clin Infect Dis* 2003; 37:e41-e43